Carbon-13 NMR Studies of Platinum(II) Complexes. 2. Chelate Ring Conformations and Internal Rotamer Distributions of Complexes of Methyl-Substituted Glycines

LUTHER E. ERICKSON,*[1a] JOSEPH E. SARNESKI,[1b] and CHARLES N. REILLEY[1b]

Received October 6, 1977

A detailed characterization of the conformational properties of a series of *N*- and *C*-methyl-substituted glycine (gly) complexes of platinum(II) is reported. Both chelated complexes of the general formula $Pt(gly)Cl_2^-$ and monodentate N-bound complexes of the type $Pt(gly)(NH_3)_3^+$ have been studied. Carbon-13 NMR chemical shifts and platinum-195–carbon-13 spin–spin coupling constants reported herein have been instrumental in defining the conformational behavior of these complexes. The chelates derived from $Pt(gly)Cl_2^-$ are best described as adopting an envelope conformation in solution with methyl substitution on the carbon and nitrogen atoms causing some puckering around the C–N bond of the chelate ring. A linear regression analysis of the carbon-13 shifts of these chelates yielded additive substituent effect parameters which, in conjunction with $^3J_{Pt-C}$ coupling constants, permitted the identification of the most abundant isomers in the conformational equilibrium of a number of asymmetric chelates. In the study of the N-bound monodentate complexes, $^3J_{Pt-C}$ data presented here were combined with earlier $^3J_{Pt-H}$ and $^3J_{H-H}$ data, to yield a self-consistent, quantitative analysis and free energy differences between rotamers for a variety of methyl-substituted glycinate complexes. Conformational equilibria in both sets of complexes are most influenced by gauche interaction of methyl groups found on carbon and nitrogen atoms and much less so by interaction with other centers ($-CO_2^-$, $-Pt(NH_3)_3^{2+}$, or $-Cl^-$) in these molecules. Relative signs of $^2J_{Pt-N-H}$ and $^3J_{Pt-N-C-H}$ (opposite sign) for $Pt(gly)Cl_2^-$ and of $^2J_{Pt-N-C}$ and $^3J_{Pt-N-C-H}$ (same sign) for $Pt(gly)Cl_2^-$ and $Pt(gly)(NH_3)_3^+$ are also reported.

Introduction

In the first paper in this series, we reported carbon-13 NMR data for platninum(II) chelates of several substituted 1,2-diamines.[2] The principal finding was that $^3J_{Pt-C}$ is a sensitive indicator of chelate ring conformation. Carbons which are trans to Pt in Pt–N–C–C fragments show large coupling ($J = 50$ Hz) while those for which the dihedral angle approaches 90° show much smaller coupling ($J = 0-10$ Hz).

In this paper, we report a parallel study of platinum complexes of glycine and several substituted glycines. Both chelate complexes, **1**, and monodentate N-coordinated species, **2**, have been examined. This series is particularly interesting since proton NMR data are also available for the series,[3] so that a comparison of conformational preferences indicated by proton and carbon-13 data can be made.
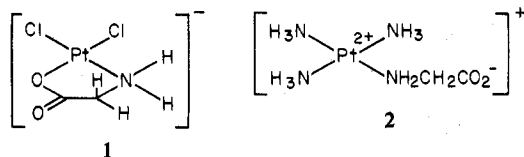
For ten chelate compounds, listed in Table I, substituent effects on chemical shifts were analyzed by the commonly employed technique of assuming additivity of effects to obtain shift parameters for α, β, γ, geminal $(CH_3)_2$, and vincinal contributions for both skeletal and CH_3 carbons.[4] For the monodentate N-coordinated species, listed in Table II, substituent parameters were determined for the α carbon only, since chemical shifts of the other carbons would be expected to depend as much on rotamer distribution as on substituent contribution.

Conformational analysis of glycinate chelates was based on Pt–C coupling constants, supplemented by previously reported three-bond vicinal Pt–H and H–H coupling constants.[3] Conformational analysis of the monodentate N-coordinated species, based on the same parameters, assumed that observed values of the three parameters are weighted averaged over the three staggered conformations associated with rotation about the N–C bond (**3a–3b–4**) and that all three parameters follow a $\cos^2 \phi$ dependence on the dihedral angle ϕ.[3,5]

3a	**4**	**3b**
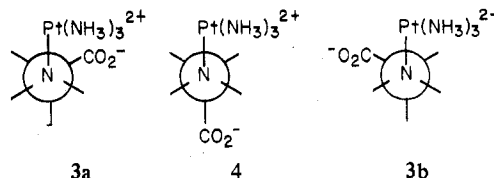
Experimental Section

Complexes of Substituted Glycines. Chelate complexes like K-[Pt(gly)Cl₂] were prepared as described earlier.[3] Complexes whose potassium salts were too insoluble to obtain good spectra were converted to soluble H^+ species by passing a saturated solution of the potassium salt through a Dowex-50 cation-exchange resin in the H^+ form and evaporating the resultant solution to dryness. After spectra of 0.5–1.0 M solutions of chelate species were recorded, the solutions were evaporated to dryness and heated to 70–80 °C with 10 M aqueous ammonia for 10–15 min to form the colorless N-coordinated species, $Pt(gly)(NH_3)_3^+$, etc., which were never actually isolated. D_2O solutions of the N-coordinated species were obtained by evaporating the reaction mixture to dryness and redissolving the solid in D_2O.

Data for *cis*-Pt(meala)Cl₂⁻ were obtained from a spectrum of an equilibrium mixture of cis and trans isomers prepared by conversion of K[Pt(meala)Cl₂] to the H^+ form after equilibration at mid-pH.[3] The spectrum of the trans isomer alone was obtained by converting the less soluble *trans*-K[Pt(meala)Cl₂] to the H^+ form and running the spectrum at low pH before significant conversion to the equilibrium mixture.

[15]N- and ^{13}C-Labeled Glycine Complexes. These compounds were synthesized from corresponding [15]N (99% enriched)- and [13]C (90% enriched)-labeled glycine. Relative signs of $^2J_{Pt-N-H}$ and $^3J_{Pt-N-C-H}$ were determined from the proton spectrum of K[Pt([15]NH₂CH₂C-O)Cl₂] freshly dissolved in 0.01 M DCl, which was recorded before NH_2 protons had a chance to exchange with D_2O solvent. Approximately 1 M solutions of K[Pt(NH₃[13]CH₂CO₂)Cl₂] and of [Pt(ND₂[13]CH₂CO₂)(ND₃)₃]Cl in D_2O were used in heteronuclear spin tickling experiments to determine relative signs of $^3J_{Pt-H}$ and $^2J_{Pt-C}$ or $^{2,3}J_{Pt-C}$ for the α carbon.

NMR Spectra. Carbon-13 NMR spectra were obtained with a Varian XL-100 NMR spectrometer as described earlier.[2]

Computer Calculations. Multiple regression analysis of chemical shift and coupling constant data was carried out with a CDC-6400 computer at the University of Arizona, using a standard linear regression program.[6]

Results

A typical carbon-13 NMR spectrum, that of Pt(dmala)Cl₂⁻, is shown in Figure 1. The spectrum consists of four equal intensity peaks which are assigned to the α carbon and three

Table I. Carbon-13 Chemical Shifts[a] and ^{195}Pt–^{13}C Coupling Constants[b] for Glycinate Chelates

Compound	Structure	N–CH$_3$	C=O	α-C	C–CH$_3$	$^3J_{HH}$[c]	$^3J_{Pt-H}$	$^4J_{Pt-H}$
Pt(gly)Cl$_2^-$			190.59[a] (46)[b]	48.33 (30)		6.5 (av)	38.5	
Pt(sarc)Cl$_2^-$		44.16 (17)	188.60 (30)	59.04 (25)		4.3 (AX) 6.6 (BX)	38.5 (H$_A$) 33.5 (H$_B$)	
Pt(dmgly)Cl$_2^-$		55.52 (14)	186.34 (15)	69.16 (22)			32.9	
Pt(ala)Cl$_2^-$			191.26 (36)	55.71 (25)	19.26 (31)	(N.O.)	28.0	<1
cis-Pt(meala)Cl$_2^-$		37.78 (21)	(N.O.)[d]	63.00 (24)	15.12 (29)	4.3	21	2.7
trans-Pt(meala)Cl$_2^-$		43.72 (22)	190.90 (28)	66.42 (23)	17.89 (11)	3.4	41.8	3.2
Pt(dmala)Cl$_2^-$		53.80 (19) 48.68 (19)	188.01 (N.O.)	72.77 (21)	13.84 (18)		27.3	3.3
Pt(aba)Cl$_2^-$			192.33 (14)	61.94 (22)	26.98 (21)			<1
Pt(meaba)Cl$_2^-$		38.37 (23)	190.77 (20)	67.83 (20)	22.82 (22) 26.52 (10)			2.8 (H$_A$) 2.2 (H$_B$)
Pt(dmaba)Cl$_2^-$		48.68 (23)	189.91 (~5)	74.56 (18)	22.25 (10)			3.1

[a] In ppm vs. Me$_4$Si. [b] Values for J_{Pt-C} (Hz) are given in parentheses next to the chemical shift of the corresponding carbon. [c] $^3J_{H-N-C-H}$. [d] N.O. is resonance line not observed due to insufficient signal to noise.

methyl carbons. Each of the peaks is flanked by the doublet due to coupling of carbon-13 nuclei to platinum-195 in ^{195}Pt(dmala)Cl$_2^-$; the spacing between doublet components is J_{Pt-C}. The much weaker signal for the C=O carbon at 188.01 ppm is not shown on this trace. Carbonyl carbon signals were often too weak to determine J_{Pt-C} reliably.

Chemical shifts and coupling constants are summarized in Tables I and II. Chemical shifts were measured with respect to internal dioxane and were converted to the Me$_4$Si scale by assigning a shift of 67.73 ppm to dioxane. The more positive shifts are more downfield. Shifts are reported to 0.01 ppm and are reproducible from sample to sample to within 0.1 ppm. Coupling constants are reported to the nearest Hz. Table II does not include any of the N,N-dimethyl derivatives since these ligands are too easily displaced by ammonia to permit their preparation by treatment of the dichloro chelate with ammonia. Each table also lists the platinum–proton and proton–proton coupling constants[3] required for convenient comparison in subsequent discussions.

Discussion

Platinum–Carbon Coupling Constants and Ring Conformations of Glycinate Chelates. The coupling constants between platinum and the four distinct types of ligand carbons (α-C,
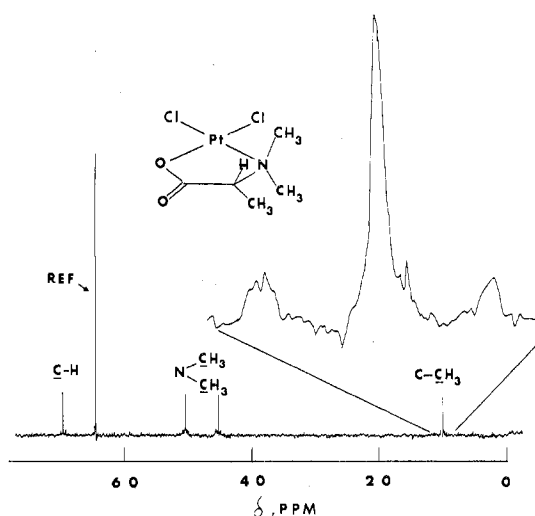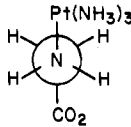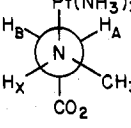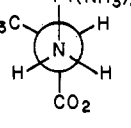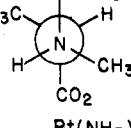

Figure 1. Carbon-13 NMR spectrum of 0.5 M H[Pt(dmala)Cl$_2$] in D$_2$O; ref = 1,4-dioxane internal reference.

C=O, C—CH$_3$, N—CH$_3$) are all influenced significantly by methyl substitution. In order to interpret ^{195}Pt–^{13}C coupling

Table II. Carbon-13 Chemical Shifts[a] and ^{195}Pt–^{13}C Coupling Constants[b] for Monodentate N-Coordinated Glycinates

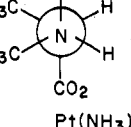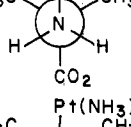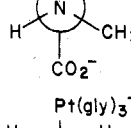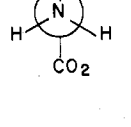| Compound	Structure	N–CH$_3$	C=O	α-C	C–CH$_3$	$^3J_{H-H}$[c]	$^3J_{Pt-H}$	$^4J_{Pt-H}$
Pt(gly)(NH$_3$)$_3$$^+$			175.82[a] (30)[b]	50.12 (17)		N.O.	37.5	
Pt(sarc)(NH$_3$)$_3$$^+$		42.77 (16)	175.27 (17)	60.23 (14)		5.2 (AX) 7.2 (BX)	52.8 (H$_A$) 27.6 (H$_B$)	
Pt(ala)(NH$_3$)$_3$$^+$			179.95 (16)	58.05 (16)	21.26 (42)	N.O.	23.6	<1
(R,R)-Pt(meala)(NH$_3$)$_3$$^+$		42.99 (19)	178.57 (N.O.)[d]	66.38 (10)	20.67 (23)	9.0	30	<1
(S,R)-Pt(meala)(NH$_3$)$_3$$^+$		38.80 (18)	179.87 (N.O.)	66.06 (14)	17.06 (35)	9.6	30	7.0
Pt(aba)(NH$_3$)$_3$$^+$			181.54 (N.O.)	62.93 (14)	28.17 (30)			~1.5
Pt(meaba)(NH$_3$)$_3$$^+$		37.30 (N.O.)	177.66 (N.O.)	64.43 (N.O.)	26.34 (N.O.) 23.19 (N.O.)			<1 (H$_A$) 3.2 (H$_B$)
Pt(gly)$_4$$^{2-}$			176.62 (26)	50.15 (18)			42	

[a] In ppm vs. Me$_4$Si. [b] Values for J_{Pt-C} (Hz) are given in parentheses next to the chemical shift of the corresponding carbon. [c] $^3J_{H-N-C-H}$. [d] N.O. is resonance line not observed due to insufficient signal to noise.

constants, it is important to recognize the differences in numbers and types of bonds between platinum and the four ligand carbons. N—CH$_3$ groups are separated from platinum by two bonds, so that the coupling constant for N—CH$_3$ carbons can be denoted $^2J_{Pt-C}$. Similarly, the C—CH$_3$ carbons are separated from platinum by three bonds; corresponding coupling constants are denoted $^3J_{Pt-C}$. This notation ignores the possibility of significant four-bond coupling between Pt and the C—CH$_3$ carbon via the carboxyl group. However, for C=O and α-C, dual-path coupling should be considered, since each carbon is separated from Pt by two and three bonds by two different paths. For C=O, the two-bond path is Pt–O–C, the three-bond path Pt–N–C–C; for the α-C, the two-bond path is Pt–N–C, the three-bond path Pt–O–C–C as in **5**. The corresponding coupling constants are appropriately
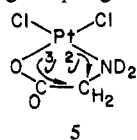
designated $^{2,3}J_{Pt-C}$. A similar mechanism was proposed earlier to account for J_{Pt-C} data in skeletal carbons of ethylenediamine platinum chelates for which two-bond and three-bond contributions of opposite sign from the two paths apparently cancel to produce negligible coupling.[2] For glycinate chelates, $^{2,3}J$ values are substantial for almost all members of the series and are especially large for Pt(gly)Cl$_2$$^-$ itself. We will distinguish between the two dual-path coupling constants by denoting the coupling for the carboxyl carbon as $^{2,3}J_{Pt-O-C}$ and for α-C as $^{2,3}J_{Pt-N-C}$ to indicate which atom is connected to the carbon being referred to. A discussion of multipath coupling effects and J_{Pt-C} data for skeletal ring carbons will be taken up in a later section.

The effect of methyl substitution on $^2J_{Pt-C}$ for N–CH$_3$ chelates is relatively small. This is not unexpected since the chelate ring conformation should not greatly affect geminal coupling. The decrease in magnitude from 17 Hz for Pt-(sarc)Cl$_2$$^-$ to 14 Hz for Pt(dmgly)Cl$_2$$^-$ is consistent with the observations for N-methyl substitution in ethylenediamine platinum(II) chelates.[2] However, substitution at the α-C leads

to a small increase in $^2J_{Pt-C}$, so that $^2J_{Pt-C}$ is larger for both isomers of Pt(meala)Cl$_2^-$ (21 and 22 Hz) than for Pt(sarc)Cl$_2^-$ (17 Hz) and is larger for Pt(dmala)Cl$_2^-$ (19 Hz) than for Pt(dmgly)Cl$_2^-$ (14 Hz). The largest observed values are for Pt(meaba)Cl$_2^-$ (23 Hz) and Pt(dmaba)Cl$_2^-$ (23 Hz). The latter values approach most closely the value found for typical *gem*-N(CH$_3$)$_2$ carbons in ethylenediamine complexes (30 Hz).[2]

It has been shown earlier that the magnitude of vicinal Pt-N-C-C coupling constants are determined by a Karplus-like dihedral angle relation so that $^3J_{Pt-C}$ for C-CH$_3$ carbons can be used to determine the preferred conformation for asymmetric chelates.[2] Based on an estimated $^3J_{PtC}$ of 50 Hz in a trans coupling orientation, an α-methyl substituent on a planar glycinate chelate ring would have a dihedral angle of 120° and should give rise to a $^3J_{PtC}$ of 12 Hz. In the case of Pt(ala)Cl$_2^-$, for which $^{2,3}J_{Pt-C}$ coupling to ring carbons suggests definite distortion from planarity, the comparatively large value of $^3J_{Pt-C}$ for C-CH$_3$ (31 Hz) requires that the ring be deformed in a sense that, on the time average, makes C-CH$_3$ more equatorial and C-H more axial. By contrast, for symmetric Pt(aba)Cl$_2^-$, in which the deformation is more severe and axial and equatorial orientations are equally probable, $^3J_{Pt-C}$ is only 21 Hz, which could be interpreted as resulting from equal contributions from equatorial ($\sim$35 Hz) and axial ($\sim$5 Hz) orientations. On that basis, the difference in $^3J_{Pt-C}$ for the two isomers of Pt(meala)Cl$_2^-$ reflects a preference for equatorial methyl for the cis isomer ($^3J_{Pt-C} = $ 29 Hz) and an axial methyl for the trans isomer ($^3J_{Pt-C} = 11$ Hz), while the intermediate value for Pt(dmala)Cl$_2^-$ 18 Hz) indicates less preference for either axial or equatorial methyl orientation. Similarly, the substantial difference between the two C-methyl couplings of Pt(meaba)Cl$_2^-$ (22 and 10 Hz) requires preference for ring deformation which produces an equatorial orientation for the upfield C-CH$_3$ ($J = 22$ Hz). From an analysis of the carbon-13 chemical shifts described in a following section this C-methyl carbon is found to be cis to the N-methyl group.

The conformational preferences of asymmetric ligands indicated by these data generally agree very well with those proposed earlier on the basis of the proton NMR data.[3] Conclusions based on $^3J_{Pt-H}$ for all four alanine ligands correspond to those based on $^3J_{Pt-C}$ values. However, our earlier suggestion that $^4J_{Pt-H}$ values of C-CH$_3$ might reflect the degree of ring deformation of low-energy conformations appears to be questionable.

Platinum–Carbon Coupling Constants and Rotamer Population Distributions of Monodentate N-Coordinated Glycinates. In our earlier analysis of rotamer distributions of N-coordinated species,[3] we assumed a cos$^2 \phi$ dihedral angle dependence for $^3J_{Pt-H}$, $^3J_{H-H}$, and $^4J_{Pt-H}$ (to C-CH$_3$ protons) to estimate relative populations of the three rotamers associated with rotation about the C-N bond. Similar assumptions about the dihedral angle dependence of $^3J_{Pt-C}$ for C-CH$_3$ carbons can be invoked to refine these estimates without using the $^4J_{Pt-H}$ data. The internal consistency of the results obtained from the three different vicinal coupling constants adds credence to the assumptions introduced and casts doubt on the validity of our earlier conclusion that $^4J_{Pt-H}$ to C-CH$_3$ protons is a reliable indicator of Pt-N-C-C dihedral angle.[3]

Relative populations of the three rotamers of each of the N-coordinated glycinates are listed in Table III along with calculated and observed values for the three vicinal coupling constants used to estimate these populations. Entries are also included for a population distribution which consists exclusively of the low-energy rotamer and for a uniform distribution of all three rotamers to illustrate the sensitivity of the observed coupling constants to rotamer distribution.

The rotamer populations were calculated by the following procedures: We assumed that $^3J_{Pt-H}$, $^3J_{H-H}$, and $^3J_{Pt-C}$ are each proportional to cos$^2 \phi$, where ϕ is the dihedral angle for the corresponding three-bond fragment. With this assumption, the coupling constant for rotamers in which i and j are gauche is (cos^2 60°)$J_{ij}^{tr} = 0.25J_{ij}^{tr}$, where J_{ij}^{tr} is the value for $\phi = 180°$. The observed couplings were then expressed in terms of trans couplings and fractional populations, f_1, f_2, and $f_3 = 1 - f_1 - f_2$. Where f_1, f_2, and f_3 denote fractional populations of rotamers I, II, and III, respectively, in Table III. For example, the four observed coupling constants of Pt(sarc)(NH$_3$)$_3$$^+$ are given by

$$J_{Pt-H_A} = (0.25 + 0.75f_1)J_{PtH}{}^{tr} = 52.8 \tag{1}$$

$$J_{Pt-H_B} = (1 - 0.75f_1 - 0.75f_2)J_{PtH}{}^{tr} = 27.6 \tag{2}$$

$$J_{H-H}(AX) = (0.25 + 0.75f_2)J_{HH}{}^{tr} = 5.2 \tag{3}$$

$$J_{H-H}(BX) = (0.25 + 0.75f_1)J_{HH}{}^{tr} = 7.2 \tag{4}$$

Solution of these simultaneous equations yields the fractional populations given in Table III and values for $J_{HH}^{tr} = 10.8$ Hz and $J_{PtH}^{tr} = 79.0$ Hz.

In a similar way, the six observed values for $^3J_{PtH}$, $^3J_{PtC}$, and $^3J_{HH}$ of the two methylalanine isomers were expressed in terms of the three trans coupling constants and four (two for each compound) fractional populations, a total of seven parameters. Using $J_{PtH}^{tr} = 79$ and $J_{HH}^{tr} = 10.8$ Hz, the sarcosine values, and eliminating J_{PtC}^{tr} from the two expressions for J_{PtC} gave five equations in the four f_i's, from which fractional populations and $J_{PtC}^{tr} = 46.7$ Hz were obtained by a multiple regression analysis. However, when both J_{HH}^{tr} and J_{PtC}^{tr} were treated as unknown parameters with $J_{PtH}^{tr} = 79.0$ Hz, the fractional populations, calculated as exact solutions to the four resulting equations, were somewhat different, while $J_{PtC}^{tr} = 49.8$ Hz and $J_{HH}^{tr} = 13.6$ Hz. Finally, fractional rotamer populations of the two isomers were recalculated from the six observed J's on the basis of a multiple regression analysis using $J_{PtH}^{tr} = 79$ Hz, $J_{PtC}^{tr} = 50$ Hz, and $J_{HH}^{tr} = 12$ Hz, a value intermediate between the 10.8 obtained from the exact solution of the sarcosine equations and the 13.6 obtained from an exact solution of the methylalanine equations. This procedure, though admittedly somewhat arbitrary, yielded a set of calculated J's in which the deviation between calculated and observed J's is distributed uniformly among the J's and the standard error in the f_i's is about 0.04. The relative rotamer populations for the methylalanines given in Table III were obtained by this approach.

With J_{ij}^{tr} values for the three coupling constants calculated from the sarcosine and methylalanine data, relative rotamer populations of the alanine and α-aminoisobutyric acid complexes were then calculated by the same approach. For ala, two independent equations can be written involving two observed coupling constants, J_{PtC} (42 Hz) and J_{PtH} (23.6 Hz), the corresponding trans values, 50 and 79 Hz, respectively, and the fractional populations of two of the three rotamers. For the aba complex two independent equations can be written to express J_{PtC} for the two distinct methyl groups in terms of J_{PtC}^{tr} and two fractional populations. The results of these calculations are summarized in Table III. Table III also includes rotamer populations for the glycine complex calculated as described above.

Relative free energies of the three rotamers were calculated from the fractional populations f_i and f_j by eq 5, with $T = $

$$f_j/f_i = \exp(G_i + G_j/RT) \tag{5}$$

308°. These free energies, measured relative to the lowest energy rotamer, are included in Table III.

The relative rotamer populations and free energies in Table III consistently indicate that the Pt(NH$_3$)$_3$$^{2+}$-CH$_3$ gauche

Table III. Rotamer Population Distribution of Monodentate N-Coordinated Glycinates

Compound	Rotamer structures	Rel pop I	Rel pop II	Rel pop III	$^3J_{PtH}$	$^3J_{HH}$	$^3J_{PtC}$	Rel free energies I	Rel free energies II	Rel free energies III
gly	I, II, III	0 / 0.147 / $^1/_3$	1 / 0.716 / $^1/_3$	0 / 0.147 / $^1/_3$	19.8 / 37.4 (37.5) / 39.5			0.97	0	0.97
ala	I, II, III	0 / 0.065 / $^1/_3$	0 / 0.148 / $^1/_3$	1 / 0.787 / $^1/_3$	19.8 / 23.6 (23.6) / 39.5		50 / 42 (42) / 25	1.50	1.00	0
sarc	I, II, III	1 / 0.558 / $^1/_3$	0 / 0.310 / $^1/_3$	0 / 0.132 / $^1/_3$	$H_A = 79$ / $H_B = 19.8$; $H_A = 52.8 (52.8)$ / $H_B = 27.6 (27.6)$; $H_A = 39.5$ / $H_B = 39.5$	$H_A = 2.7$ / $H_B = 10.8$; $H_A = 5.2 (5.2)$ / $H_B = 7.2 (7.2)$; $H_A = 5.4$ / $H_B = 5.4$		0	0.35	0.86
R,R-meala	I, II, III	0 / 0.150 / $^1/_3$	1 / 0.627 / $^1/_3$	0 / 0.223 / $^1/_3$	19.8 / 28.7 (30) / 39.5	12 / 8.7 (9.0) / 6	12.5 / 20.9 (23) / 25	0.86	0	0.62
S,R-meala	I, II, III	0 / 0.172 / $^1/_3$	0 / 0.149 / $^1/_3$	1 / 0.679 / $^1/_3$	19.8 / 30.0 (30.0) / 39.5	12 / 9.1 (9.6) / 6	50 / 37.9 (35) / 25	0.82	0.91	0
aba	I, II, III	0.5 / 0.467 / $^1/_3$	0 / 0.066 / $^1/_3$	0.5 / 0.467 / $^1/_3$			31.3 / 30 (30) / 25.0	0	1.17	0

Coupling constants,^{a} Hz — Calcd (obsd)

^{a} Three different values are given for each coupling constant of each compound to indicate the sensitivity of coupling constants to relative population changes. They correspond, respectively, to (a) the most stable rotamer only, (b) the most probable distribution, and (c) equal population of all three rotamers.

Table IV. Gauche Interaction Free Energies Calculated from Relative Populations of Monodentate N-Coordinated Glycines in [Pt(gly)(NH$_3$)$_3$]$^+$-Type Complexes

Parameter	ΔG, kcal/mol	Standard error
ΔG(Pt(NH$_3$)$_3$$^{2+}$–CO$_2$$^-$)	0.63	0.20
ΔG(Pt(NH$_3$)$_3$$^{2+}$–CH$_3$)	1.39	0.22
ΔG(CH$_3$–CO$_2$$^-$)	0.62	0.25
ΔG(CH$_3$–CH$_3$)	1.14	0.30

interaction is more repulsive than the Pt(NH$_3$)$_3$$^{2+}$–CO$_2$$^-$ gauche interaction but that both interactions are more repulsive than gauche interactions involving the Pt(NH$_3$)$_3$$^{2+}$ with N–H or C–H. Thus, for Pt(gly)(NH$_3$)$_3$$^+$, conformation II, with Pt(NH$_3$)$_3$$^{2+}$ and CO$_2$$^-$ trans, is most stable. For Pt(ala)-(NH$_3$)$_3$$^+$, conformation I, with two unfavorable gauche interactions, is least stable, while conformation III is favored over II. The favored rotamer III places the methyl group trans to the platinum center in an orientation which is thought[3,7] to be conducive to a strong ^4J coupling of the methyl protons with the platinum nucleus. The lack of any discernible $^4J_{PtH}$ in the methyl resonance of Pt(NH$_3$)$_3$(ala)$^+$ is surprising.

Continuing through the series, for Pt(sarc)(NH$_3$)$_3$$^+$, conformation I, with CO$_2$$^-$ gauche to Pt(NH$_3$)$_3$$^{2+}$, is preferred over II, wherein the CO$_2$$^-$ and CH$_3$ are gauche. For the two isomers of Pt(meala)(NH$_3$)$_3$$^+$, the rotamers with only two unfavorable gauche interactions are more abundant than conformations with three such interactions. Of the higher energy rotamers, conformation I, with Pt(NH$_3$)$_3$$^{2+}$ gauche to CO$_2$$^-$, prevails over II which has Pt(NH$_3$)$_3$$^{2+}$ gauche to CH$_3$ for (S,R)-Pt(meala)(NH$_3$)$_3$$^+$. In the R,R isomer the energy difference between the less favored rotamers I and III, both of which have Pt-(NH$_3$)$_3$$^{2+}$ gauche to CO$_2$$^-$, is much smaller than for the corresponding higher energy forms in the R,S complex. Finally, for Pt(aba)(NH$_3$)$_3$$^+$, I and III with gauche Pt-(NH$_3$)$_3$$^{2+}$–CO$_2$$^-$ groups are favored over II in which Pt-(NH$_3$)$_3$$^{2+}$ is trans to CO$_2$$^-$.

Finally approximate energy contributions for unfavorable gauche interactions involving Pt(NH$_3$)$_3$$^{2+}$, CO$_2$$^-$, and CH$_3$ were estimated by assuming that the energy differences between rotamers is dominated by these interactions. Thus, $\Delta G_I - \Delta G_{II}$ = $\Delta G_{III} - \Delta G_{II}$ for Pt(gly)(NH$_3$)$_3$$^+$ = ΔG(Pt(NH$_3$)$_3$$^{2+}$–CO$_2$$^-$) etc. For the six compounds in Table III, this assumption yields ten independent equations in the four free energy terms denoted ΔG(Pt(NH$_3$)$_3$$^{2+}$–CO$_2$$^-$), ΔG(Pt(NH$_3$)$_3$$^{2+}$–CH$_3$), ΔG-(CH$_3$–CO$_2$$^-$) and ΔG(CH$_3$–CH$_3$). A multiple regression analysis of these data yielded the values for these four parameters that are listed in Table IV. The relatively small standard deviations suggest that the energy parameters are reasonably reliable. However, the poorest fit between calculated and observed energy differences is obtained for Pt-(gly)(NH$_3$)$_3$$^+$, for which ΔG = 0.97 kcal/mol (vs. 0.56 calculated by the regression fit). In any case, the values indicate the CH$_3$–CH$_3$ and Pt(NH$_3$)$_3$$^{2+}$–CH$_3$ interactions are particularly unfavorable. The former value (1.14 kcal/mol) is somewhat larger than the energy difference between the rotamers of n-butane (0.8 kcal/mol).[8] This might reflect the closer approach of the two methyl groups in the platinum complexes because the C–N bond is shorter than the C–C bond in butane. And the smallest gauche interaction is indicated for the gauche Pt(NH$_3$)$_3$$^{2+}$–CO$_2$$^-$ interaction, which may be stabilized by charge effects or by intramolecular hydrogen bonding between amine hydrogens and the carboxyl oxygens, as shown in Figure 3. As Figure 3 suggests, a complete conformational analysis of these compounds should also take into account rotation of the Pt(NH$_3$)$_3$$^{2+}$ moiety about the Pt–N bond. This is particularly important when the amino acid is an N-substituted glycine, for which stabilization by hydrogen bonding can compete with unfavorable steric interaction

between N–CH$_3$ and NH$_3$ groups of the Pt(NH$_3$)$_3$$^{2+}$ moiety.

Vicinal coupling between Pt and carboxyl carbons might also be expected to be sensitive to ligand conformation. Unfortunately, the low intensity of the carbonyl carbon signals due to signal saturation prevented us from obtaining sufficient data to permit any useful quantitative analysis. However, the relative values of $^3J_{Pt–C}$ for Pt(gly)(NH$_3$)$_3$$^+$ (30 Hz) and Pt(sarc)(NH$_3$)$_3$$^+$ (17 Hz) are consistent with the expectation that such coupling should be larger when the CO$_2$$^-$ group is trans to platinum. Interestingly, a similar conformation is suggested for the glycinate moiety in both Pt(gly)(NH$_3$)$_3$$^+$ and Pt(gly)$_4$$^{2-}$ in which all four glycinate ligands are N coordinated.[9]

Platinum–Carbon Coupling Constants of Glycinate Chelate Ring Carbon Atoms: Multipath Coupling. Our earlier results[2] for the coupling of platinum-195 nuclei with skeletal ring carbons of five-membered chelate rings formed by various ethylenediamines and platinum(II) exhibited the peculiar feature that $J_{Pt–C}$ appeared to be absent (or very small, <4 Hz) for most skeletal carbon atoms in the series. The most consistent explanation of these results (in view of sizable $^2J_{Pt–C}$ and $^3J_{Pt–C}$ values in many other similar molecules) involved the hypothesis of distinct, additive coupling paths between the platinum center and the skeletal carbons in five-membered rings, one ^2J path and one ^3J path. Available data suggested that $^2J_{Pt–C}$ and $^3J_{Pt–C}$ might be of similar magnitude for these ring carbons and opposite in sign so that direct additivity could lead to a cancellation effect with resultant loss of observable ^{195}Pt–^{13}C coupling.

Ring carbons of the five-membered glycine chelate rings can also be thought to undergo spin-coupling interaction with platinum-195 by two paths. These ring carbons exhibit $J_{Pt–C}$ values sensitive to methyl substitution on the ligand skeleton. For the carboxyl carbon, $^{2,3}J_{Pt–O–C}$ values range from 46 Hz for Pt(gly)Cl$_2$$^-$ to ~5 Hz for Pt(dmaba)Cl$_2$$^-$. A sharp decrease in $^{2,3}J_{Pt–O–C}$ of the glycine chelate from 46 to 30 to 15 Hz with N-methyl substitution is paralleled by a corresponding sharp decrease from 46 to 36 to 14 Hz with C-methyl substitution.

An attractive explanation for these changes is that they reflect a transition from a nearly planar ring for Pt(gly)Cl$_2$$^-$ to more puckered rings for the gem-dimethyl derivatives. This interpretation is based on the assumption that $^{2,3}J_{Pt–O–C}$ for carbonyl carbons of Pt(gly)Cl$_2$$^-$ should be dominated by a large positive contribution from the three-bond Pt–N–C–C path which has a dihedral angle close to 0°; this is partially offset by a much smaller, relatively conformation independent, two-bond coupling via the Pt–O–C path. A parallel argument can be invoked to account for the much smaller, but significant, change in $^{2,3}J_{Pt–N–C}$ for the α carbon (from 30 to 25 to 22 Hz for both series). The smaller value for α-carbon coupling relative to the carboxyl carbon coupling in the glycine chelate suggests either that positive coupling via the vicinal three-bond Pt–O–C–C path is smaller than vicinal coupling via the three-bond Pt–N–C–C path or that the negative geminal contribution from Pt–O–C is greater than that from Pt–O–C, or both. In any case, the much larger decrease in $^{2,3}J_{Pt–O–C}$ for carboxyl carbons upon methyl substitution suggests that the increased puckering (deviation from planarity where $^3J_{Pt–C}$ is expected to be maximum) has more influence on the dihedral angle of the Pt–N–C–C fragment, ϕ_1; the smaller changes in $^{2,3}J_{Pt–N–C}$ imply less change in the Pt–O–C–C dihedral angle, ϕ_2. These observations then suggest that the deformed rings of the methyl-substituted glycines are more nearly of the envelope type (A) than of the puckered type (B), as shown in Figure 2.

A test of the proposed dual-path coupling scheme for the α carbon of chelated Pt(gly)Cl$_2$$^-$ can be made by determining the relative signs of Pt–C and Pt–H coupling constants.
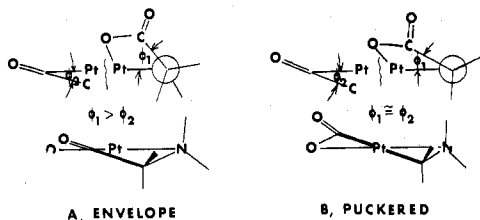
Figure 2. Possible conformations of glycinate chelate rings and corresponding dihedral angles.
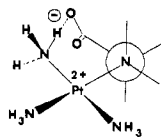

Figure 3. Hydrogen bond stabilization of gauche $Pt(NH_3)_3{}^{2+}-CO_2{}^-$ rotamers of $Pt(gly)(NH_3)_3{}^+$ ions.

According to the proposed model, monodentate $Pt(NH_3)_3$-$(gly)^+$ and chelated $Pt(gly)Cl_2{}^-$ would be expected to have opposite signs for coupling of the platinum nucleus with the α carbon of glycine. In monodentate $Pt(NH_3)_3(gly)^+$ $^2J_{Pt-C}$ is expected to be negative as is found for most ^2J couplings of nuclei with positive gyromagnetic ratios, e.g, for $^2J_{Hg-C}$ in $Hg(CH_2CH_2CH_2CH_3)_2$.[11] Similarily, $^3J_{Pt-H}$ is expected to be positive as in $[Pt(CH_2CH_3)_3Cl]_4$[12] and $^3J_{Hg-H}$ in $Hg(CH_2-CH_3)_2$,[13] as well as most vicinal systems. In the chelate, **5**, however, where the platinum and α carbon can couple via both two- and three-bond paths, the sign of $^{2,3}J_{Pt-C}$ for this coupling would be positive if dominated by the vicinal interaction. By contrast, the coupling of platinum to the α hydrogens for both compounds is expected to be positive, since the four-bond path through the oxygen of the chelate should be insignificant. Thus the model predicts $^3J_{Pt-H}$ and $^2J_{Pt-C}$ to have the same relative sign in the chelate and opposite signs in the monodentate complex, $Pt(NH_3)_3(gly)^+$.

The prediction can be tested using well-documented double resonance (spin tickling) techniques. In molecules containing three distinct intercoupled nuclei (e.g., in the glycine platinum complexes, for which an AMX_2 spectrum is possible, were A $= {}^{195}Pt$, M $= {}^{13}C$, X $= {}^1H$) the relative signs of any two coupling constants can be obtained by observing the effects on the NMR resonances of any one nucleus of simultaneous low-amplitude irradiation at specific resonance lines of a second nucleus.[14,15] In effect, the third nucleus (the one not decoupled or observed) acts as the marker to relate signs of coupling constants of itself to the other two nuclei. So, for example, by irradiating specific proton lines and observing the resultant effects in the carbon-13 spectrum of $Pt(NH_3)_3(gly)^+$, one could determine the relative signs of $^3J_{Pt-N-C-H}$ and $^2J_{Pt-N-C}$. A similar experiment can be performed for the chelate Pt-$(gly)Cl_2{}^-$.

The three coupling nuclei required in this case are depicted for the monodentate N-bonded complex in D_2O as (A) $^{195}Pt-ND_2-{}^{13}C^1H_2-COO^-$ (0.37%). Unfortunately, natural abundances of the elements constituting these species require that other isotopically distinct complexes (B–D) are present in greater abundance as shown below, where ^0Pt represents all naturally occurring platinum isotopes, all with $I =$ 0: (B) $^0Pt-ND_2-{}^{13}C^1H-COO^-$ (0.73%), (C) $^{195}Pt-ND_2-{}^{12}C^1H-COO^-$ (33.4%), (D) $^0Pt-ND_2-{}^{12}C^1H-COO^-$ (65.5%). The relative percentages of the four distinct isotopic species (A–D) in an ordinary preparation of a glycine platinum chelate are given in parentheses. Therefore, samples of ^{13}C-enriched (90% ^{13}C) $Pt(gly)Cl_2{}^-$ and $Pt(NH_3)(gly)^+$ were prepared by using ^{13}C-enriched (at the α carbon) glycine ligand.

The proton NMR spectrum of the monodentate N-bound $(ND_3)_3Pt(ND_3{}^{13}CH_2COO^-)^+$ is shown in Figure 4a. Res-
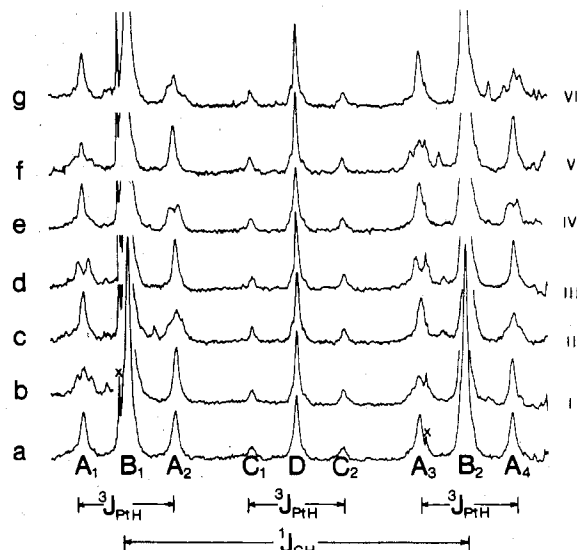

Figure 4. (a) 100-MHz FT proton NMR spectrum of $Pt(ND_3)_3(gly)^+$ (α-C 90% ^{13}C labeled) in D_2O. Labels attached to various transitions refer to isotopically different molecules described in text A, B, C, and D; $\times$ indicates impurity peak; $^3J_{Pt-H} = 30$ Hz and $J_{CH} = 140$ Hz. (b)–(g) $^1H-{}^{13}C$ spin tickling double resonance experiments where lines A_5 through A_{10} in carbon-13 spectrum (Figure 5) of $Pt(ND_3)(gly)^+$ are successively irradiated with low-amplitude single-frequency radiation. Roman numeral designations at right of each spectrum refer to lines labeled such as in Figure 5.
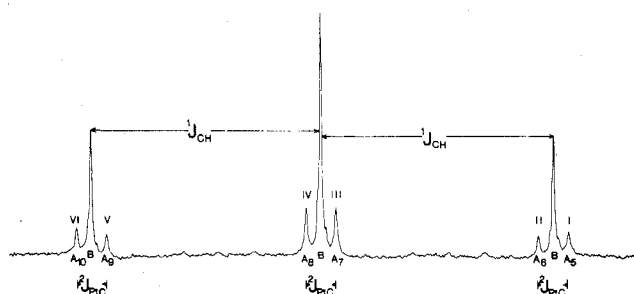

Figure 5. Proton-undecoupled 25.2-MHz ^{13}C NMR spectrum of methylene carbon signals (carbonyl signal not shown) of Pt-$(ND_3)(gly)^+$. Designations refer to molecules A and B described in text. Coupling constants: $^1J_{CH} = 140$ Hz and $^2J_{Pt-C} = 18$ Hz. Irradiation frequencies used for various lines: $A_5 = 25, 161, 308$ Hz; $A_6 = 25, 161, 326$ Hz; $A_7 = 25, 161, 448$ Hz; $A_8 = 25, 161, 466$ Hz; $A_9 = 25, 161, 588$ Hz; $A_{10} = 25, 161, 606$ Hz.

onances due to isotopically distinct species A–D (abundance calculated for 90% α-^{13}C label: A $= 30.4$%, B $= 59.6$%, C $= 3.4$%, D $= 6.6$%) are labeled. The corresponding proton undecoupled ^{13}C spectrum of the α-carbon resonances in labeled $(ND_3)_3Pt(ND_2{}^{13}CH_2COO^-)^+$ is given in Figure 5. In this spectrum only two types of molecules, A and B, contribute; molecules containing the spin $^1/_2$ ^{195}Pt isotope (A) give rise to the satellites around the three major lines which are due to $^1J_{C-H}$ in the $^{13}CH_2$ moiety B. The ^1H and proton undecoupled ^{13}C NMR spectra for the labeled chelate $Pt(gly)Cl_2{}^-$ are very similar in appearance. Only the magnitudes of the various coupling ($^1J_{C-H} = 142$ Hz, $^3J_{Pt-H} = 38$ Hz, and $^{2,3}J_{Pt-NC}$ $= 30$ Hz) are different.

Using the spin Hamiltonian and known coupling constants the energy levels for the various transitions in an AMX_2 system ($^{195}Pt^{13}C^1H_2$) were derived for situations where J_{Pt-N-C} and $J_{Pt-N-C-H}$ had the same and opposite signs. For the two possible relative signs of J_{Pt-N-C} and $J_{Pt-N-C-H}$ different lines are expected to undergo splitting. The predicted results of low-amplitude single frequency irradiation of each of the ^{13}C transitions in $Pt(ND_3)_3(gly-\alpha^{13}C)^+$, labeled A_5–A_{10} in Figure 5, which should be visible in the proton NMR spectrum as

Table V. Summary of the Predicted Splittings Observable in Proton NMR Resonances upon Single-Frequency ^{13}C Tickling Experiments for the ^{195}Pt–N–^{13}C–^{1}H$_2$ Fragment in Platinum Glycine Complexes

Rel signs of	^{13}C line irradiated					
$^3J_{PtH}$ and $^2J_{PtC}$	A$_5$	A$_6$	A$_7$	A$_8$	A$_9$	A$_{10}$
Same sign	A$_2$A$_4$	A$_1$A$_3$	A$_2$A$_4$	A$_1$A$_3$	A$_2$A$_4$	A$_1$A$_3$
Opposite signs	A$_1$A$_3$	A$_2$A$_4$	A$_1$A$_3$	A$_2$A$_4$	A$_1$A$_3$	A$_2$A$_4$

splitting of lines A$_1$–A$_4$ in Figure 4 are summarized in Table V.

The results of the ^{1}H–^{13}C tickling experiments on Pt-(ND$_3$)$_3$(gly)$^+$ are depicted in Figure 4b–g. Irradiation of the low-frequency component (A$_5$, A$_7$, A$_9$) of each of the three doublets in the carbon-13 spectrum produces splitting of *only* the high-frequency lines (A$_1$ and A$_3$) of the platinum satellites in the proton spectrum. Irradiation of the high-frequency components in the ^{13}C spectrum (A$_6$, A$_8$, A$_{10}$) causes splitting of only the A$_2$ and A$_4$ proton lines. Furthermore, irradiation of lines A$_7$ and A$_8$ in the ^{13}C spectrum produces a doublet in the tickled proton lines while irradiation of all other ^{13}C lines gives a triplet splitting in the tickled spectra in agreement with the predictions of Freeman and Anderson.[16] These results require that $^3J_{Pt–N–C–H}$ and $^2J_{Pt–N–C}$ have opposite signs. Since $^3J_{Pt–H}$ in Pt(NH$_3$)$_3$(gly)$^+$ is almost certainly positive, $^2J_{Pt–N–C}$ is then negative.

Analogous experiments on Pt(gly)Cl$_2^-$ demonstrate identical tickling effects as depicted in Figure 4, which requires that $^{2,3}J_{Pt–N–C}$ and $^3J_{Pt–N–C–H}$ in this molecule also have opposite signs. Thus, assuming $^3J_{Pt–H}$ is positive, $^{2,3}J_{Pt–N–C}$ for the α-C of the chelate complex, like $^2J_{Pt–N–C}$ for the N-coordinated species, is also negative.

This result seems to be at odds with the predictions of the dual-path coupling scheme outlined earlier since $^{2,3}J_{Pt–N–C}$ was expected to be dominated by a substantial positive contribution via the Pt–O–C–C path. However, coupling through the Pt–O–C–C bonds may be much weaker than through Pt–N–C bonds, so that the observed coupling may be dominated by the negative $^2J_{Pt–C}$ contribution. The smooth decrease with N-methyl substitution of $^{2,3}J_{Pt–C}$ for α-C is paralleled by a smooth increase of $^2J_{Pt–C}$ for N–CH$_3$ carbons. If the three-bond contribution to α-C coupling is very small, these trends might both result from small changes in Pt–N–C bond angles. As the Pt–N–CH$_3$ angle increases, the Pt–N–CH$_2$ angle would be expected to decrease, and vice versa. Thus, the apparent contradiction between the dual-path coupling model and the sign determination may simply reflect the very small contribution to $^{2,3}J_{Pt–C}$ from the Pt–O–C–C path. If this is indeed the case, the much larger decrease in $^{2,3}J_{Pt–C}$ for the carbonyl carbon with methyl substitution could still be explained in terms of increased ring puckering with substitution. This would require that $^{2,3}J_{Pt–C}$ coupling to α-C and carbonyl carbon are opposite in sign with $^{2,3}J_{Pt–O–C}$ being positive and $^{2,3}J_{Pt–N–C}$ being negative. Unfortunately, a spin tickling experiment parallel to the one done on Pt(ND$_2$–^{13}CH$_2$CO$_2$)Cl$_2^-$ probably cannot be done on Pt(ND$_2$–CH$_2$^{13}CO$_2$)Cl$_2^-$ because $^2J_{C–H}$ would probably be too small to observe significant splitting.

Measurement of $J_{Pt–O–C}$ for the carboxyl carbon of the six-membered ring of the chelate of β-alanine would provide evidence for the suggestion that such coupling is very small. Unfortunately, relatively low solubility and weak carboxyl carbon signals have so far prevented reliable determination of $^2J_{Pt–O–C}$. However, no discernible satellites were observed in the spectra that have been recorded.

Additional evidence for the relative sign assignment in these systems is provided by a determination of the relative signs of $^2J_{Pt–N–H}$ vs. $^3J_{Pt–N–C–H}$ in the chelate Pt(gly)Cl$_2^-$. We prepared this complex from ligand 99% labeled with ^{15}N and

Table VI. Carbon-13 Chemical Shift Substituent Parameters for Pt(gly)Cl$_2^-$ and Its Methyl Derivatives

Carbon	Correlation parameter	No. of cases	Value ± std error, ppm
α-C	δ_0, unsubstituted α-carbon shift	9	48.35 ± 0.22
	δ_α, effect of C-methyl substitution	6	7.50 ± 0.23
	δ_β, effect of N-methyl substitution	6	10.76 ± 0.25
	$\delta_{\alpha gem}$, effect of geminal C(CH$_3$)$_2$	2	−1.59 ± 0.38
	$\delta_{\beta gem}$, effect of geminal N(CH$_3$)$_2$	3	−0.80 ± 0.41
	δ_{gau}, effect of vicinal gauche methyls	3	−3.88 ± 0.21
	Overall root-mean-square deviation	9	± 0.15
C–CH$_3$	δ_0, unsubstituted methyl carbon shift	8	19.06 ± 0.14
	δ_β, effect of second methyl group	4	8.08 ± 0.14
	$\delta_{\alpha cis}$, effect of cis-N-CH$_3$	4	−4.02 ± 0.14
	$\delta_{\alpha tr}$, effect of trans-N-CH$_3$	4	−1.05 ± 0.14
	Overall root-mean-square deviation	8	± 0.14
N–CH$_3$	δ_0, unsubstituted N-methyl shift	8	44.16 ± 0.60
	δ_β, effect of second N-methyl	4	10.42 ± 0.60
	$\delta_{\alpha cis}$, effect of cis-C-CH$_3$	4	−5.68 ± 0.60
	$\delta_{\alpha tr}$, effect of trans-CH$_3$	4	−0.16 ± 0.60
	Overall root-mean-square deviation	8	± 0.60
C=O	δ_0, unsubstituted carbonyl shift	8	190.28 ± 0.42
	δ_β, effect of C-CH$_3$	5	1.32 ± 0.28
	δ_α, effect of N-CH$_3$	5	−1.65 ± 0.26
	Overall root-mean-square deviation	8	± 0.50

observed an AA′BB′MX spectrum in the 60-MHz proton NMR spectrum of this chelate due to the presence of the isotopic moiety ^{195}Pt(^{1}H$_2$^{15}N–C^{1}H$_2$–CO$_2$)Cl$_2^-$. Computer simulation techniques confirmed that $^2J_{Pt–H}$ and $^3J_{Pt–H}$ are opposite sign in this case which is consistent with the normal observations in σ-bonded networks.[12,13,17] This determination adds weight to our assumption that $^3J_{Pt–H}$ for Pt(gly)Cl$_2^-$ is positive (while $^2J_{Pt–H}$ is negative).

An alternative explanation for the unexpected negative sign for $^{2,3}J_{Pt–N–C}$ is that coupling paths in such cyclic species are not truly additive and have a much more complex functionality. A thorough treatment of multipath coupling effects is to our knowledge lacking in the literature, although some allusion to these phenomena has been made.[18] This anomalous result may also occur because of the presence of the unsaturated carbon of the carbonyl carbon in the three-bond coupling path (Pt–O–C=O–C) which if it reversed the sign of $^3J_{Pt–C}$ via this path would reinforce the negative coupling expected for the two-bond path Pt–ND$_2$–CH$_2$. We are not aware of any sign determination of $J_{Pt–C}$ across a bound carboxylate moiety.
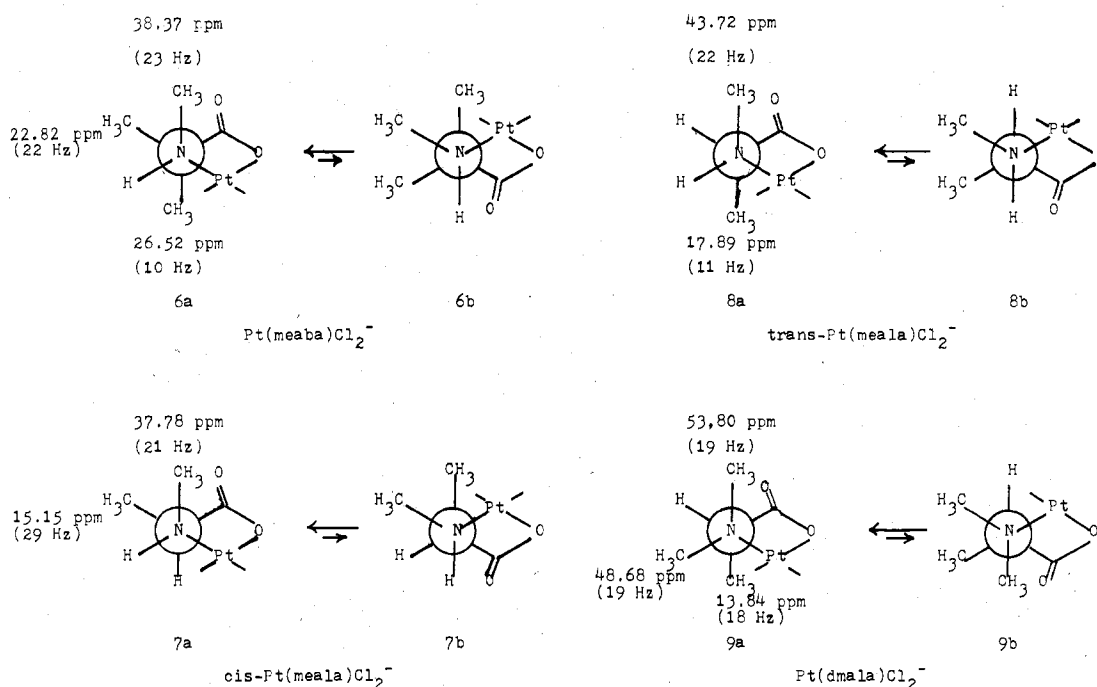
Chemical Shifts of Glycinate Chelates. Following the approach introduced by Grant and co-workers to account for substituent effects on carbon-13 chemical shifts of hydrocarbons,[4] we assumed that the chemical shifts of each of the four types of carbons (α-C, C—CH$_3$, N—CH$_3$, and C=O) of the glycinate chelates could be expressed as a linear combination of substituent parameters of the form

$$\delta = \delta_0 + \Sigma n_i \delta_i \qquad (6)$$

where δ_0 is the shift of the parent structure, δ_i is the contribution to the shift from substituent i, and n_i is the number of ith substituents. A linear regression analysis was used to determine the values of the m parameters which gave the smallest deviation between calculated and observed shifts for the entire set of values. Results of the analyses are summarized in Table VI.

Preliminary inspection of the data suggested the inclusion of different parameters for the four different types of carbons. For the α carbon, six parameters were included in the regression analysis. These included δ_0, the contribution from the unsubstituted compound (48.35 vs. 49.33 ppm experimentally measured for Pt(gly)Cl$_2^-$) δ_α and δ_β, the effects of α- and β-methyl substituents, $\delta_{\alpha gem}$ and $\delta_{\beta gem}$, the smaller negative effects of geminal C(CH$_3$)$_2$ or N(CH$_3$)$_2$ configu-

38.37 ppm
(23 Hz)

22.82 ppm
(22 Hz)

26.52 ppm
(10 Hz)

6a   6b

Pt(meaba)Cl₂⁻

43.72 ppm
(22 Hz)

17.89 ppm
(11 Hz)

8a   8b

trans-Pt(meala)Cl₂⁻

37.78 ppm
(21 Hz)

15.15 ppm
(29 Hz)

7a   7b

cis-Pt(meala)Cl₂⁻

53.80 ppm
(19 Hz)

48.68 ppm
(19 Hz)

13.84 ppm
(18 Hz)

9a   9b

Pt(dmala)Cl₂⁻

Figure 6. Description of the preferred conformations of some of the methyl-substituted glycinate chelates. Superimposed on the favored conformer is found carbon-13 chemical shift data (ppm) and $^3J_{PtC}$ (Hz) for the methyl substituents.

rations, and δ_{gau} which takes into account gauche interactions of N-methyl and C-methyl substituents needed particularly to distinguish the substantial difference between cis- and trans-Pt(meala)Cl₂⁻ shifts. The root-mean-square difference between δ calculated from the values for these parameters and δ observed is 0.15 ppm for the nine cases. Standard errors of the individual parameters are somewhat larger (0.21–0.41 ppm).

For C–CH₃ carbons, only four parameters were included. These are δ_0, the value for the unsubstituted species (19.06 vs. 19.26 ppm found for Pt(ala)Cl₂⁻, δ_β, the β effect of another methyl substituted on the α carbon and $\delta_{\gamma cis}$ and $\delta_{\gamma tr}$, the γ-effect parameters for cis and trans N-methyl subsitution. A parallel set of parameters was used for the effect of N and C–CH₃ substitution on N–CH₃ shifts, with comparable results (standard error 0.60 vs. 0.14 ppm for C–CH₃ shifts). Finally, for the carbonyl shifts which covered a much smaller group range, only two parameters, δ_β for the β effect of C–CH₃ substitution and δ_γ for the γ effect of N–CH₃ substitution, were included, in addition to δ_0, the shift for the parent compound (190.28 vs. 190.59 ppm found for Pt(gly)Cl₂⁻). The multiple regression yielded an overall standard error of 0.50 ppm.

The general pattern of substituent parameters closely parallels that observed for hydrocarbon fragments, modified somewhat by the replacement of one carbon by a nitrogen. The effect of methyl substitution on the α-carbon chemical shift (7.50 ppm) is somewhat smaller than the 9.1 ppm typical of hydrocarbons. The effect on the C-methyl chemical shift of substitution of a second methyl group on the α carbon atom, δ_β (8.08 ppm), is less than the 9.4 ppm shift found in hydrocarbons.[4] By contrast, the analogous β effect of N-methyl substitution on N–CH₃ chemical shift (10.42 ppm) or on the α-carbon chemical shift (10.76 ppm) is significantly larger than the 9.4 ppm of hydrocarbons. Perhaps, the shorter N–C bond length compared to the C–C bond length alters the interaction between the two carbons in C–N–CH₃ fragments compared to C–C–CH₃ fragments. The negative γ effect of both an N–CH₃ on a C–CH₃ and vice versa is strongly dependent on stereochemistry, with $\delta_{\gamma cis}$ (−4.02 and −5.68 ppm, respectively) having gauche interactions being much larger than $\delta_{\gamma tr}$ (−1.05

and −0.16 ppm) where the methyl groups are not gauche to one another. These values are comparable to the −5.4 and 0 ppm calculated for axial and equatorial CH₃ γ effects in cyclohexanes.[4] Similarly, the effect of geminal C(CH₃)₂ and N(CH₃)₂ (−1.59 and −0.80 ppm) on the α-carbon shift parallels the effect of α- and β-dimethyl substitutions in cyclohexane (−3.4 and −1.2 ppm); also, the effect of vicinal gauche CH₃–C–N–CH₃ on the α-carbon chemical shifts (−3.88 ppm) is comparable to the −2.3 and −3.1 ppm effects calculated for vicinal diequatorial and vicinal axial–equatorial orientations (both having gauche methyl interactions) of cyclohexane, respectively. Finally, the β and γ effects on the carbonyl carbon shifts (1.32 and −1.65 ppm, respectively) are comparable to values reported for several saturated aldehydes and ketones (β ≃ 2 and γ ≃ −1 ppm).[4]

An understanding of these shift parameters can be used in conjunction with $^3J_{PtC}$ data discussed earlier to gain a description of the predominant conformation of certain of the glycinate chelates (6–9) shown in Figure 6. In Pt(meaba)Cl₂⁻ the pseudo-axial character of the N-methyl substituent is seen from the mutual γ-gauche upfield shift experienced by the N-methyl carbon (relative to 8a and similar to 7a) and the pseudo-equatorial C-methyl carbon (relative to axial C–CH₃ in 6a). This conformation appears to avoid the unfavorable gauche interaction of the N-methyl group and both C-methyl substituents. In cis-Pt(meala)Cl₂⁻ (7) once again the gauche disposition of methyl groups in the favored conformer accounts for the upfield shifts of the C- and N-methyl carbon resonances relative to the favored trans-Pt(meala)Cl₂⁻ conformer 8a. This finding is interesting because in the alternative axial C-methyl conformer, 7b, a similar gauche methyl interaction appears to be present, yet the fairly large $^3J_{Pt-C}$ (29 Hz) experienced by the methyl carbon resonance indicates that conformer 7a which places the platinum nucleus and C-methyl carbon in a trans vicinal orientation is definitely favored. By similar argument, in the complex trans-Pt(meala)Cl₂⁻ the diaxial conformer 8a appears to be dominant because of the relative downfield nature of the carbon-13 shifts of the methyl substituents and low $^3J_{Pt-C}$ (11 Hz) of the C-methyl group. Available $^3J_{Pt-H}$ data[3] for the meala chelates 7 and 8 support these ideas. Perhaps the diequatorial methyl orientation 8b

**Table VII.** Chemical Shift Parameters for the α Carbon of Methyl Derivatives of $Pt(gly)(NH_3)_3^+$

Correlation parameter	No. of cases	Value ± std error	Chelate values
δ_0, unsubstituted (glycine)	7	51.80 ± 2.60	48.35
δ_α, effect of C–CH$_3$	5	7.20 ± 2.97	7.50
δ_β, effect of N–CH$_3$	4	6.75 ± 2.50	10.76
δ_{gem}, effect of *gem*-C(CH$_3$)$_2$	2	5.89 ± 4.99	-1.59

is disfavored in this case because such an orientation places four substituents (two methyl groups, carbonyl oxygen, and chloride ion bound to platinum) in a similar plane around the complex. In the complex $Pt(dmala)Cl_2^-$, **9**, the 5 ppm difference in *N*-methyl chemical shifts similar to the difference in axial *N*-methyl shifts in **7a** and **8a** would seem to be due to one *N*-methyl group experiencing a γ gauche upfield shift and the other none. This situation occurs in **9a** whereas in **9b** both *N*-methyl groups have a γ-gauche interaction. These data suggest that **9a** is more abundant then **9b**; yet the $^3J_{PtC}$ of 18 Hz is much more typical of an average equatorial–axial coupling constant for the *C*-methyl group as described earlier and may indicate that this conformer predominance is not as great as in the meala chelates **8** and **9**.

Chemical Shifts of Monodentate N-Coordinated Glycinates. The factors which were identified as being important in determining chemical shifts of chelated glycinates can also be invoked to account for the effect of methyl substitution on carbon shifts of monodentate N-coordinated glycinates, the parent compound being $Pt(gly)(NH_3)_3^+$. However, for these N-coordinated species, the situation is complicated by changes in rotamer populations resulting from methyl substitution, which have already been discussed. A complete analysis might attempt to estimate chemical shifts for all three rotamers of each methylglycine complex. However, the range of shifts is too small, the number of compounds too few, and the relative rotamer populations too inaccurately known to permit such a complete analysis. Since we are unable to take into account the rotamer distributions we will base the discussion below on comparisons of shifts of preferred rotamers of these species which exist primarily in one rotamer.

Of the four types of carbons (α-C, C—CH$_3$, N—CH$_3$, and C=O) the α-carbon shifts should be least influenced by changes in rotamer populations and most susceptible to analysis in terms of the additive contribution model used for the chelate ligands. Results of such an analysis for the seven compounds in Table II ($Pt(gly)_4^{2-}$ omitted) are summaried in Table VII. The values for the N-coordinated species agree reasonably well with the corresponding values for the chelates which are included in Table IV for convenient reference. However, they are less precise.

A comparison of N–CH$_3$ and C–CH$_3$ shifts for sarosine, alanine, and the isomers of *N*-methylalanine **10–13** supports the previous assignment of preferred rotamers for these species based on coupling constants. Since $Pt(sarc)(NH_3)_3^+$, **10**, $Pt(ala)(NH_3^+)^+$, **11**, and (S,R)-$Pt(meala)(NH_3)_3^+$, **12**, all have CO_2^- gauche to $Pt(NH_3)_3^{2+}$ in the preferred conformation, the large upfield shift of both N–CH$_3$ (3.97 ppm) and C–CH$_3$ (4.20 ppm) of (S,R)-$Pt(meala)(NH_3)_3^+$ relative to $Pt(sarc)(NH_3)_3^+$ and $Pt(ala)(NH_3)_3^+$ can be attributed mainly to the γ effect of the gauche methyls. The much smaller upfield shift of N–CH$_3$ (0.48 ppm) and C–CH$_3$ (0.59 ppm) of (R,R)-$Pt(meala)(NH_3)_3^+$, **13**, suggests that the γ effect of a gauche $Pt(NH_3)_3^{2+}$ or CO_2^- group is much smaller than that of a methyl group. Further evidence for this conclusion is provided by the fact that the addition of another C–CH$_3$ to $Pt(ala)(NH_3)_3^+$ to form $Pt(aba)(NH_3)_3^+$ produces the 7 ppm shift predicted for α-CH$_3$ substitution, in spite of the fact that one of the methyl groups of the latter must always be gauche to the $Pt(NH_3)_3^{2+}$.

10   11   12   13
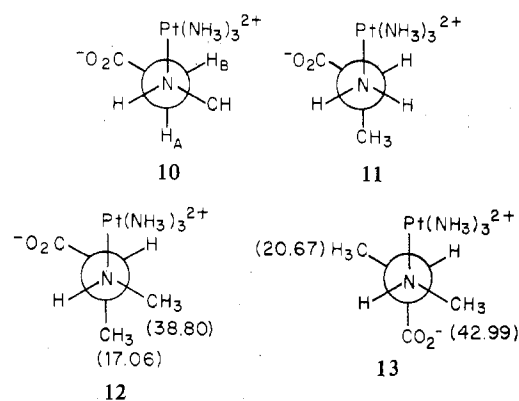
Conclusion

In these amino acid complexes, like those of the diamines,[2] the carbon-13 NMR spectra provide valuable clues to the detailed structures of ions in solution. On the basis of data for these two series and for the six-membered rings formed by 1,3-diaminopropanes,[19] we have been able to investigate structural and equilibrium properties of platinum complexes of more complex ligands, including potentially tridentate triamine ligands,[20] and the amino acids proline and pipecolic acid (2-carboxpiperidine).[21] In the latter case, proton NMR spectra, even at high fields, are too complex to permit convenient analysis.

References and Notes

(1) (a) Grinnell College. (b) The University of North Carolina.
(2) L. E. Erickson, J. E. Sarneski, and C. N. Reilley, *Inorg. Chem.*, **14**, 3007 (1975).
(3) L. E. Erickson, M. D. Erickson, and B. L. Smith, *Inorg. Chem.*, **12**, 412 (1973).
(4) D. M. Grant and B. V. Cheney, *J. Am. Chem. Soc.*, **89**, 5315 (1967); D. K. Dalling and D. N. Grant, *ibid.*, **89**, 6612 (1967), and other references cited therein.
(5) N. Karplus, *J. Chem. Phys.*, **30**, 11 (1959); *J. Am. Chem. Soc.*, **85**, 2870 (1963).
(6) BMDO2, available from "Biomedical Computer Programs", University of California Press, Berkeley, Calif., 1973.
(7) T. G. Appleton and J. R. Hall, *Inorg. Chem.*, **9**, 1807 (1970); **10**, 1717 (1971); **11**, 117 (1972).
(8) E. Eliel, N. L. Allinger, S. J. Angyal, and G. A. Morrison, "Conformational Analysis", Wiley, New York, N.Y., 1964, p 9.
(9) L. E. Erickson, J. W. McDonald, J. K. Howie, and R. P. Clow, *J. Am. Chem. Soc.*, **90**, 6371 (1968).
(10) J. B. Stothers and P. C. Lauterbur, *Can. J. Chem.*, **42**, 1563 (1964).
(11) F. J. Wiegert and J. D. Roberts, *J. Am. Chem. Soc.*, **91**, 4940 (1969).
(12) S. F. A. Kettle, *J. Chem. Soc.*, 6664 (1965).
(13) P. T. Narasimhan and M. T. Rogers, *J. Chem. Phys.*, **34**, 1049 (1961).
(14) J. W. Emsley, J. Feeney, and L. H. Sutcliffe, "High Resolution Nuclear Magnetic Resonance Spectroscopy", Vol. 1, Pergamon Press, London, 1965, pp 466–475.
(15) W. McFarlane and R. F. M. White, "Techniques of High Resolution Nuclear Magnetic Resonance Spectroscopy", CRC Press, Cleveland, Ohio, 1972, pp 90–95.
(16) R. Freeman and W. A. Anderson, *J. Chem. Phys.*, **37**, 2053 (1962).
(17) J. W. Emsley, J. Feeney, and L. H. Sutcliffe, "High Resolution Nuclear Magnetic Resonance Spectroscopy", Vol. 2, Pergamon Press, London, 1966, p 688.

(18) A. K. Jameson, presented at First Rocky Mountain Regional Meeting of the American Chemical Society, Fort Collins, Col., July 1972, Abstracts No. Physical-17.

(19) J. E. Sarneski, C. N. Reilley, and L. E. Erickson, in preparation.

(20) J. E. Sarneski, A. T. McPhail, K. D. Onan, L. E. Erickson, and C. N. Reilley, *J. Am. Chem. Soc.*, **99**, 7376 (1977).

(21) L. E. Erickson, J. E. Sarneski, and C. N. Reilley, *Inorg. Chem.*, submitted for publication.

Carbon-13 NMR Studies of Platinum(II) Complexes. 3. Investigation of the Configuration and Ligand Conformation of Complexes of the Cyclic α-Amino Acids Proline and Pipecolic Acid

LUTHER E. ERICKSON,*[1a] JOSEPH E. SARNESKI,[1b] and CHARLES N. REILLEY[1b]

Received October 6, 1977

Carbon-13 NMR spectral data are reported for platinum(II) complexes of both chelated [Pt(amino acid)Cl₂]⁻ and N-coordinated [Pt(amino acid)(NH₃)₃]⁺ species, where amino acid is proline or pipecolic acid. Both types of complexes can exist in distinguishable isomer forms, cis- and trans-fused rings for the chelates and diastereomers, due to the presence of two asymmetric centers for the N-bound monodentate complexes. However, in all cases except [Pt(pip)Cl₂]⁻, where a 2:1 ratio of cis to trans isomers is found, one isomer is strongly preferred. [13]C chemical shifts were used to make assignments of isomer structures. As in decalins, cis-fused rings exhibit ^{13}C chemical shifts more upfield than their trans-fused isomers. $^3J_{Pt-C}$ data support these assignments and permit assessment of preferred conformations of coordinated ligands. Isomer and conformer preferences can be reconciled by comparison with established distribution of rotamers in previously characterized platinum(II) complexes of N-methylalanine. A contrast of the steric forces involved in determining conformer preferences in the chelates and monodentate complexes is presented. Evidence for an envelope structure for the five-membered ring in the monodentate proline complex is given. Contrasts between the conformation and isomer preferences of these ligands in square-planar platinum(II) and octahedral cobalt(III) complexes are related to the influence of apical ligands in the latter.

Introduction

In an earlier paper in this series we reported carbon-13 NMR data for platinum(II) complexes of glycine and the *C*- and *N*-methylglycines.[2] Conclusions about the preferred conformations of five-membered glycinate chelate rings and corresponding N-coordinated unidentate species were drawn from [195]Pt–[13]C coupling constants for ligand carbons and from comparison of proton[3] and carbon-13 NMR data for the series.

In this paper, we report a parallel ^{13}C NMR investigation of the stereochemistry of platinum(II) complexes of the cyclic amino acids proline (pro) and pipecolic acid (2-piperidine-carboxylic acid = pip). For these asymmetric ligands, as for *N*-methylalanine, coordination by Pt introduces a second chiral center at the coordinated nitrogen atom so that diastereomers are possible for both chelate and N-coordinated species. Ring closure to form glycinate-type chelate rings with the pro and pip ligands leads to chelates having fused rings in which ligand–ring constraints influence the chelate structures that are possible. For the proline chelate [Pt(pro)Cl₂]⁻,[4] only a cis isomer, **1**, can be formed because of the constraint provided by the fused five-membered rings. On the other hand, both cis and trans isomers of the monodentate N-coordinated species [Pt(pro)(NH₃)₃]⁺, **2** and **3**, are possible, in principle. For pipecolic acid complexes, both trans and cis isomers of [Pt-(pip)Cl₂]⁻, **4** and **5**, can be formed, with the cis configuration possessing two distinct conformers related by a ring-inversion equilibrium, **5a** ⇌ **5b**. The corresponding cis (*R,R* or *S,S*) and trans (*R,S* or *S,R*) isomers of [Pt(pip)(NH₃)₃]⁺, **6a, b** and **7a, b**, are also possible.

Earlier workers[5,6] have used circular dichroism spectra to establish the stereochemistry of these three asymmetric ligands when they are chelated in octahedral complexes of the type [Co(NH₃)₄(aa)]²⁺, where aa is an amino acid anion ligand. They concluded that stereospecific binding occurs for all three
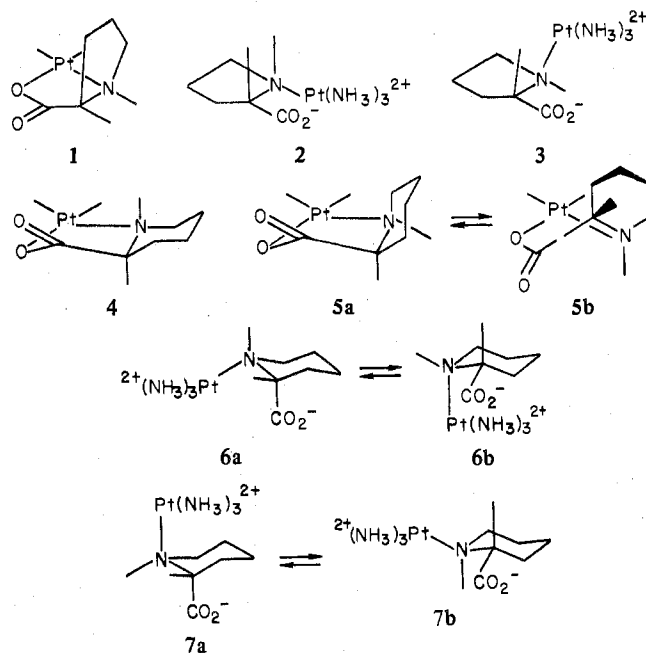
chiral ligands. For proline, the cis structure (like **1**) is favored. However, for pipecolic acid the trans form (as in **4**) prevails, while only the *R,S* chelate of *N*-methyl-L-alanine (with N–CH₃ and C–CH₃ trans) was observed. In view of the different steric constraints present in the octahedral complexes because of axial ligation, which are not present in square-planar complexes, significant differences in isomer distributions of Co(III) and Pt(II) complexes could be expected.

The characterization of isomers of the square-planar platinum(II) complexes of these asymmetric ligands by [13]C